Korean J. Chem. Eng., 34(7), 2072-2078 (2017)
DOI: 10.1007/s11814-017-0096-z

pISSN: 0256-1115
eISSN: 1975-7220

Formation and stability study of silver nano-particles in aqueous and organic medium

Md. Niamul Haque*, Sunghyun Kwon,†, and Daechul Cho*****

*Department of Ocean System Engineering, College of Marine Science, Gyeongsang National University, Cheondaegukchi-gil 38, Tongyeong, Gyeongnam 53064, Korea
**Department of Marine Environmental Engineering, College of Marine Science, Engineering Research Institute (ERI) Gyeongsang National University, Cheondaegukchi-gil 38, Tongyeong, Gyeongnam 53064, Korea
***Department of Energy and Environmental Engineering, Soonchunhyang University, 22, Soonchunhyang-ro, Asan-si, Chungcheongnam-do 31538, Korea
(*Received 23 November 2016 • accepted 4 April 2017*)

Abstract−Colloidal silver nanoparticles were obtained by chemical reduction of silver nitrate in water and organic solvent with sodium borohydride. The effects of oxidant, reducing agent, stabilizer, and temperature, during the growth of silver nanoparticles were discussed. As the reaction proceeded in aqueous medium a characteristic plasmon absorption peak between 390-420 nm appeared as presence of silver nanoparticles. The peak intensities and shifting (blue or red) were altered in accordance with some applied factors. The formed silver nanoparticles were found to be with particles size range from 3 to 20 nm. The change rates of Ag^+ ions to Ag^0 in aqueous and organic solvent are strongly temperature dependent, although reduction can take place at room temperature. The silver nano-colloid with negative zeta potential also has been confirmed to be more stable. Obtained nanoparticles were characterized by UV-vis spectrophotometer, particle analyzer for zeta (ζ) potential, polydispersity index (PDI), and transmission electron microscope (TEM).

Keywords: UV-vis Spectra, Chemical Reduction, Silver Nanoparticles, Poly (vinyl) Pyro-lidone (PVP), Transmission Electron Microscope (TEM), Polydispersity Index (PDI)

INTRODUCTION

Nanotechnology is dedicated to the creation, improvement, and utility of nanoscales structures for advanced studies. Among them, a noble metal silver nanoparticle is an emerging field of interdisciplinary research [2]. Nano phasic and nanostructured materials are receiving a great deal of attention for their potential for achieving specific processes and selectivity, especially in biological and pharmaceutical application [3]. The vivid colors from noble metal nano-silver were used for decorative pigments for glass [4] and ceramics [5] in ancient times. Nano-silver powder is widely used in daily life [6], medicine [7] textiles including cotton [8], wool, silk [9,10] fields for human health guaranty. Recent literature reports encouraging results about the bactericidal activity of silver nanoparticles of either a simple or composite nature [11]. Elechiguerra and coworkers [12] found that silver nanoparticles undergo a size-dependent interaction with human immunodeficiency virus type 1, preferably via binding to gp120 glycoprotein knobs. Silver nanoparticles have applications in electronics in addition to their potential use in opto-electronics, in catalysis, and as conductive inks [13,14]. Despite the fact that nanocrystalline silver powder is well utilized for micro- and nanotechnology, challenges associated with their large-scale synthesis by solution method are formidable.

Novel metal nanoparticles present bright colors because of their localized surface plasmon resonance (LSPR) features. Conduction electrons around metal nanoparticles locally oscillate at a certain frequency when light interacts with nanoparticles. The excitation of surface plasmons by light is known as LSPR [15]. The LSPR property of noble metal nanoparticles has been widely applied in many fields such as surface enhanced spectroscopy [16] and sensing [17]. The color of fabrics treated with noble metal nanoparticles depends on the shape and size of nanoparticles on the fibers [18].

Several methods have been used in the past to prepare nanostructured silver particles, including chemical reduction [19], electrochemical reduction [20], heat evaporation [21], thermal decomposition in organic solvents [22], polyol process [23], chemical and photo-reduction in reverse micelles [24], and radiation chemical reduction [25]. All these methods of preparation involve the reduction of relevant metal salts in the presence or absence of surfactants, which is necessary for controlling the growth of metal colloids through agglomeration. Various chemical and physical methods are known for preparation of silver and other metal nanoparticles. Silver nanoparticles are fabricated by the reduction of silver ions to neutral silver atoms. Silver ions are reduced by the use of reducing agents [26]. In the formation of silver nanoparticles by chemical reduction method, there are several factors that are important to prepare nanosized powder of silver. Properties of silver nanoparticles obtained by this method are affected by various parameters, such as molar concentration of R ($[AgNO_3]$/[reducing agent]) value, dispersant concentration, feed rate of reactant etc. [27]. Therefore,

†To whom correspondence should be addressed.
E-mail: shkwon@gnu.ac.kr

we considered how the parameters such as silver nitrate, sodium borohydride, polyvinyl pyrrolidine (PVP) and temperature affect the reduction process as well as size, and shape of the silver nanoparticle in aqueous and organic medium.

MATERIALS AND METHODS

1. Reagents

Silver nitrate ($AgNO_3$, >99%), sodium borohydride ($NaBH_4$, >99%), poly (vinyl-pyrrolidine) (PVP, average molecular weight 40,000), 1, 2-propanol and 2-methoxyethanol were purchased from Daejung Chemical, South Korea. All the chemicals were of analytical grade and used as received. Double distilled water was used throughout the reaction.

2. Instruments

UV-vis spectra were measured using a spectrophotometer (SHIMADZU, GENESYS 8, England, with 1 cm path length Quartz cell and graph plotted on the SigmaPlot 10.0 program). For transmission electron microscope (TEM, JEOL, JEM-1011; Japan) samples were prepared by placing a drop of working solution on a carbon coated standard copper grid (300 mesh) operating at 80 kV accelerating voltage. The particle size distribution, Zeta (ζ) potential and polydispersity index (PDI) of the silver nano particle in the colloid were measured by Zetasizer Nano S90, UK. The stability of the colloidal system is determined by magnitude of the zeta potential. The measurement of zeta potential stability is based on the direction and velocity of particles under the influence of electric field.

3. Synthesis of Silver Nano-particle

The solution of silver nitrate and reducing agents was prepared daily and stored in a dark glass bottle. In a typical process, 10-mL volume of silver nitrate (2.0 mM) was added dropwise (roughly one drop/second) into 30 ml of sodium borohydride (4.0 mM) solution, under different experimental condition (Table 1). To obtain stable silver nanoparticles, the order of reactant addition is important. The immediate silver nanoparticles aggregation will occur in reverse order of reactant addition [28]. The PVP was added in silver nitrate solution (PVP effect) and stirred until complete dissolution. The reaction mixture also was stirred vigorously on a magnetic stir plate. After the completion of entire addition, the stirring was stopped and the stir bar removed. The aqueous reaction mixtures were heated at different temperatures, such as 40, 60, 90 °C during 30 min, and the increment of the coloration including room temperature (25 °C) was observed. The samples prepared in 1, 2-propandiol and 2-methoxyethanol were also heated to 60, 90, 120 °C with a rate of heating of 4 °C/min until reaching the desired temperature. The PVP of 80 mg was added to the system for preparation of silver nanoparticle by using organic solvents.

RESULTS AND DISCUSSION

1. Effect of $AgNO_3$ Concentration

Metal nanoparticles and their bulk materials property are not the same, although they are of the same atoms. The experiments described here, silver nitrate solution and bulk sodium borohydride, were colorless. Silver nitrate was used as a starting material. The light yellow color changed to deep yellow due to the forma-

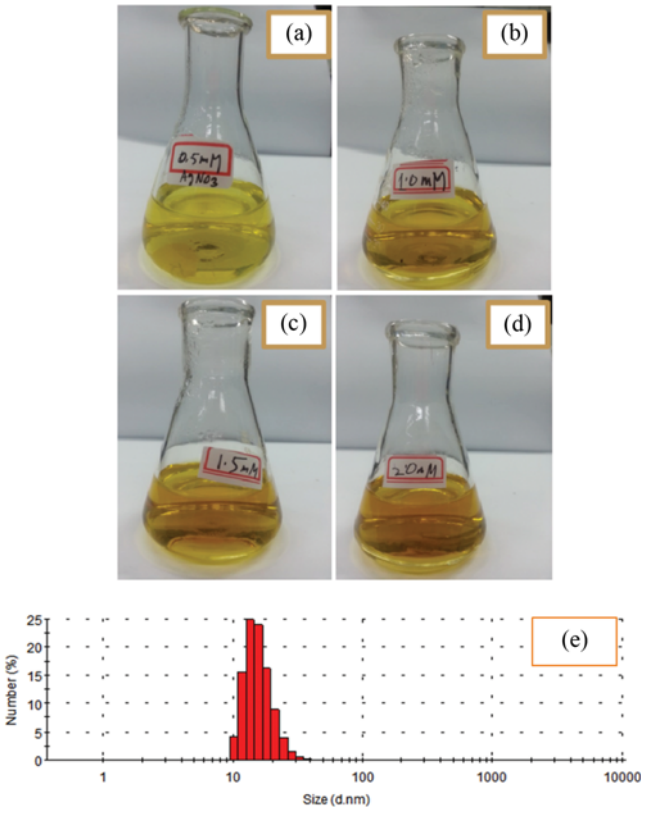

Fig. 1. Colloidal silver in various stages, (a) light yellow (0.5 mM), (b) clear yellow (1.0 mM), (c) bright yellow (1.5 mM), (d) deep yellow (2.0 mM) as growth of silver nanoparticle proceeds. (e) Silver nanoparticle size distribution of solution D (the best among samples).

Table 1. Maximum intensity and wavelength at maximum intensity at various studied conditions

$[AgNO_3]^*$ mM	λ_{max} (nm)	Abs. (a.u.)	$[NaBH_4]^*$ mM	λ_{max} (nm)	Abs. (a.u.)	$[PVP/AgNO_3]^*$ weight ratio	λ_{max} (nm)	Abs. (a.u.)	Temperature* [°C]	λ_{max} (nm)	Abs. (a.u.)
0.5	396.5	0.4093	10.0	389.0	0.5907	20.0	402.5	0.43	90	405.5	0.6324
1.0	394.5	0.5465	4.0	392.0	0.3678	5.0	403.0	0.37	60	406.5	0.4769
1.5	391.0	0.7385	2.0	397.5	0.259	2.0	405.5	0.34	40	411.0	0.1941
2.0	394.0	0.7943	1.0	394.0	0.1691	0.50	418.0	0.26	RT (25)	411.0	0.1503
*$[NaBH_4]$ is constant at 4.0 mM, RT			*$[AgNO_3]$ is constant at 1.0 mM, RT			*$[AgNO_3]/[NaBH_4]$=1 : 2 molar ration, RT			*$[AgNO_3]/[NaBH_4]$=1 : 2 molar ration		

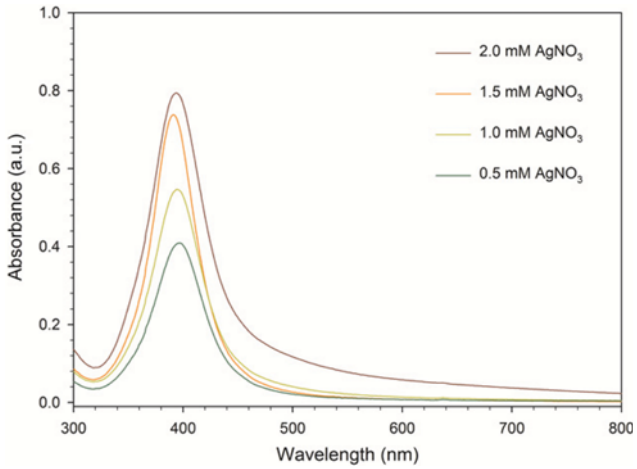

Fig. 2. UV-visible absorption spectrum of yellow colloidal Ag.

tion of silver nanoparticles with different density and size. The reaction produced visually observable well-defined stages. These are shown in Fig. 1. Sodium borohydride reduces silver nitrate, resulting in silver nanoparticles, according to the following equation [29]:

$$AgNO_3 + NaBH_4 \longrightarrow Ag + \tfrac{1}{2} H_2 + \tfrac{1}{2} B_2H_6 + NaNO_3 \quad (1)$$

The reduction of silver ion (Ag^+) in aqueous solution generally yields colloidal silver with particle diameter of several nanometers [30]. Even dilute reagents are used, because Brownian motion among the particles gives rise to agglomeration if repulsive interactions are not present. A summation of van der Waals attraction and electrostatic repulsions potential are interpreted as a term of pair in the case of particle aggregation [31]. Steric stabilization has been widely used in stabilization of nanoparticle colloid. Fig. 2 shows the UV-vis spectra of colloidal silver nanoparticles prepared with different $AgNO_3$ concentrations (0.5, 1.0, 1.5, 2.0 mM). The colors of the solutions originated according to the concentration of added $AgNO_3$ solutions. With increasing the $AgNO_3$ concentration, the color of solution changed from light yellow to deep yellow. The absorption spectra of prepared deep yellow silver colloids by reduction process showed a surface plasmon band with maximum of 397 nm, indicating the presence of spherical silver nanoparticles ranging between 10 to 24 nm with mean±SD value of 13±4 nm confirmed by the particle size analyzer (Fig. 1(e)). Metal surface like plasma comprises free electron in the conduction band and nuclei with positive charge. Near the surface of the nanoparticles, the conduction band produces plasmon resonance as a collective excitation of electrons. The vibration mode of electrons is limited to certain rate by the particle size and shape. Therefore, metallic nanoparticles have characteristic optical absorption spectra in the UV-vis region [32]. The location of absorption peak at around 394-397 nm (Table 1) in Fig. 2 is attributed to the surface plasmon excitation of silver nanospheres, indicating the formation of silver nanoparticles [33,34]. At low $AgNO_3$ concentrations (0.5, 1.0 mM), weak absorption maximum of surface plasmon peaks was observed at 396 nm and 394 nm, respectively, showing that silver nanoparticles were produced at a relatively low concentration. With increasing the $AgNO_3$ concentration, the intensity of the maximum plasmon peak increased

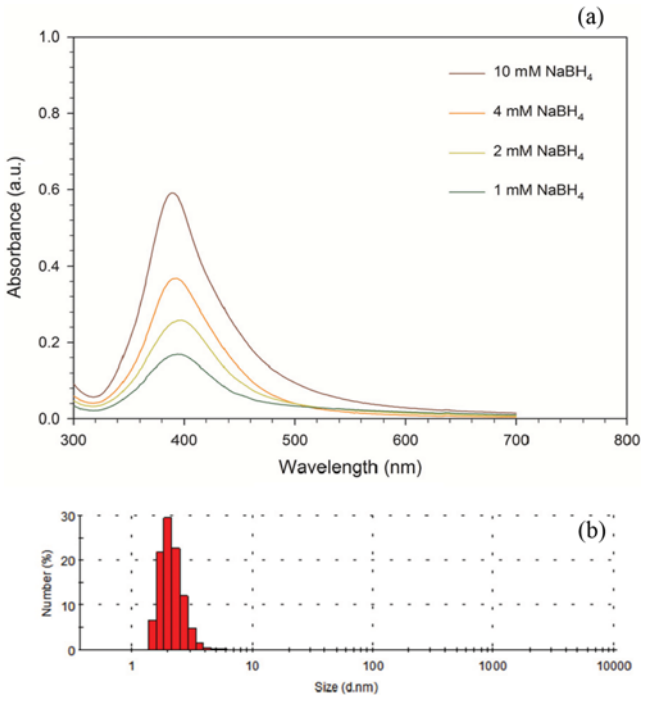

Fig. 3. UV/Vis absorption spectra of the silver nanoparticles prepared with different $NaBH_4/AgNO_3$ molar ratios. (a), particle size distribution (b).

(0.40-0.80 a.u.), indicating that higher concentrations of silver nanoparticles were formed.

2. Effect of $NaBH_4$ Concentrations

The effect of different $NaBH_4$ concentrations was monitored by the reduction reaction, carried out by varying molar concentrations of 1.0, 2.0, 4.0, 10.0 mM $NaBH_4$ at the static 1.0 mM $AgNO_3$ concentration. Fig. 3(a) shows the UV-vis spectra of studied silver colloid. Small molar ratio (1 : 1 and 2 : 1) of $NaBH_4/AgNO_3$ produced weak plasmon peak centered at 394 and 397.5 nm, with obtained absorption value of 0.17 and 0.26 a.u. (Table 1), respectively. It could be due to the formation of low concentration silver nanoparticles by insufficient reduction progress. Dispersion degree of silver nanoparticles can be known through how the spectra are developed. Narrower absorption peak means the better dispersed nanosolution [33]. The higher molar ratios of $NaBH_4/AgNO_3$ at 4 : 1 and 10 : 1 created the absorption peak at 392 and 389 nm with the intensity of 0.37 and 0.59 a.u., respectively (Table 1). Widened absorption peak indicates the gradual aggregation of silver nanoparticles. However, when the $NaBH_4/AgNO_3$ molar ratios were 10, a higher intensity absorption peak was developed. The higher intensity suggests that the silver nanoparticles were well dispersed in that stage. The results showed resemblance with [34] who reported the boron hydroxide produced through hydrolysis of $NaBH_4$ by Eq. (1). They used small concentration of $NaBH_4$. The silver nanoparticles size (diameter) varied between 2.0 to 42.0 nm with mean value of 32±4 nm (means±S.D.) for the $NaBH_4/AgNO_3$ molar ratios of 10 : 1 size nanoparticles (Fig. 3(b)). However, the aggregation state of nanoparticles depended on different $NaBH_4/AgNO_3$ molar ratios. When $NaBH_4/AgNO_3$=2, intense aggregation of silver nano-

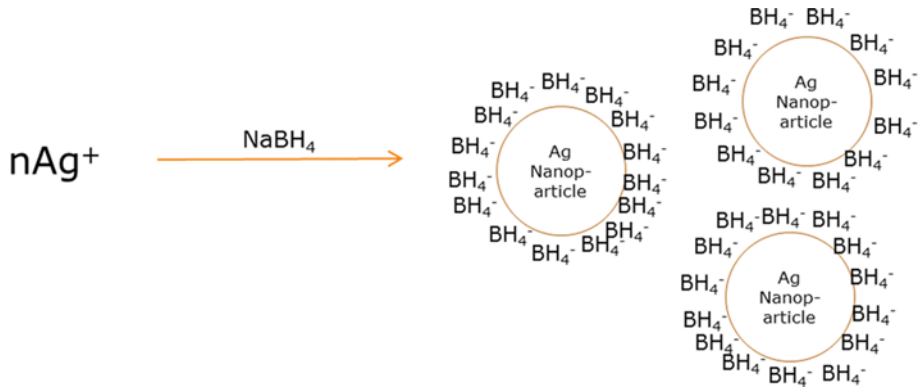

Fig. 4. Repulsive forces separate Ag nanoparticles (NP) with adsorbed borohydride layer.

particles was observed in Fig. 3(a). On the other hand, in the case of $NaBH_4/AgNO_3$=10 in Fig. 3(b), the aggregation was reduced, and the dispersion became far better. These results are well consistent with the UV-vis spectra in Fig. 3(a). The adsorption of boron hydroxide to the surface of the silver nanoparticles plays a key role in stabilizing growing silver nanoparticles by providing a particle charge as shown in Fig. 4. Initially, due to this adsorption the electron density on surface of nanoparticles was reduced and particle aggregations arose. The high quantity of $NaBH_4$ produces excess amount of BH_4^- through borohydride/water reaction and creates thick BH_4^- layer at surrounding of the silver nanoparticles. The thick BH_4^- layer protects the surface of the nanoparticle from absorbing boron hydroxide; as a result, a well dispersed solution was obtained [35]. To reduce the van der Waals attraction among the particles and prevent aggregation, BH_4^- layer was sufficient. Therefore, it would not be speculative to say that $NaBH_4$ plays an important role of reducing agent and stabilizer at the same time. The zeta potential value of the synthesized silver nanoparticles has been displayed by −17.4 mV and −42.5 mV for 2 : 1 and 10 : 1 molar ration

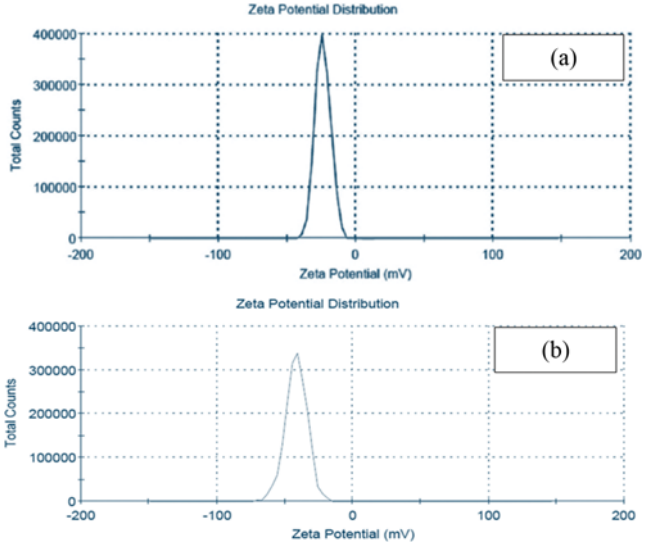

Fig. 5. Zeta(ζ) potential of silver nanoparticles solution prepared with different $NaBH_4/AgNO_3$ weight ratios. (a) $NaBH_4/AgNO_3$ =2 : 1 and (b) $NaBH_4/AgNO_3$=10 : 1.

of $NaBH_4/AgNO_3$ as shown in Fig. 5, respectively, indicating the presence of repulsion among BH_4^- charge around the synthesized silver nano. The zeta potential indicates the degree of repulsion between similarly charged particles in the dispersion [36]. The acquired value in the current research indicates that the molar ratio by 10 : 1 is stocking higher repulsion than molar ration by 2 : 1 in the colloidal dispersions. Subsequently, the polydispersity index (PDI) value is related to the colloidal stability and should be <0.3 in dynamic light scattering (DLS) technique. If the polydispersity index value of dispersions is equal and/or greater than 1, then the solution visual precipitation may arise [37]. The polydispersity index values were between 0.130 to 0.212, that is reflecting good colloidal properties, while PDI value of 0.130 was displayed by $NaBH_4/AgNO_3$=10 : 1 and 0.212 by $NaBH_4/AgNO_3$=2 : 1.

3. Effect of PVP Concentrations

Polymers are a good host material for metal nanoparticles. Polyvinyl pyrrolidone (PVP) allows a wide range of potential applications (e.g., biomedical, pharmacy, textile). Due to its optical clarity PVP is being used as a stabilizer, which facilitates investigation of the nanoparticle formation. PVP was introduced into the solution to prevent the silver nanoparticles from growth and aggregation. Fig. 6(a) shows the UV-vis spectra of colloidal silver nanoparticles with different $PVP/AgNO_3$ weight ratios by 0.5, 2, 5, and 20. We found that the intensity and width of the surface plasmon resonance are sensitive to the nanoparticle morphology. When the $PVP/AgNO_3$ weight ratios were low (0.5, 2.0), the absorption peaks became broad, indicating that silver nanoparticles were aggregated. However, at high $PVP/AgNO_3$ weight ratios (5.0, 20.0), narrow surface plasmon absorption peaks at 402 and 403 nm, respectively (Table 1) were observed, confirming the nanocrystalline characteristic and well-dispersed state of the silver particles. These results mean that when an adequate amount of PVP is used, the reaction medium is able to absorb on the surface of silver nanoparticles and disperse the electromagnetic field. The stable silver nanoparticles solution is attributed to the collective effect of van der Waals interactions, electrostatics, and steric forces [38,39]. We also found that when the ratios become higher, the resonance is blue shifted with increasing of intensity (0.26-0.48 a.u., Table 1). A blue shift implies that the surface charge density is high, as results disperse and stable solution has formed. The size of the nanoparticles varied between 2.0 to 9.0 nm with mean value of 3±2 nm (means± S.D.) (Fig. 6(b)).

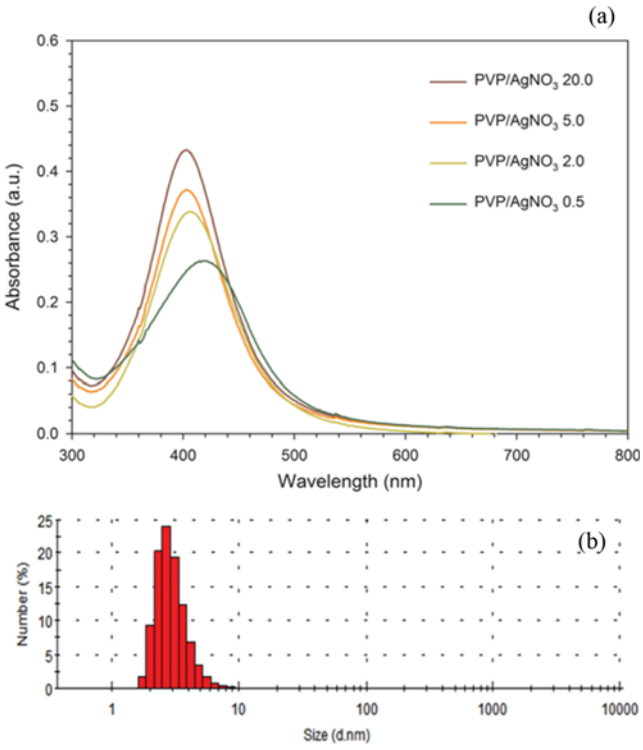

Fig. 6. UV-vis absorption spectra of the silver nanoparticles prepared with different PVP/$AgNO_3$ weight ratios (a), size distribution of silver nanoparticles for PVP/$AgNO_3$ weight ratios 20 (b).

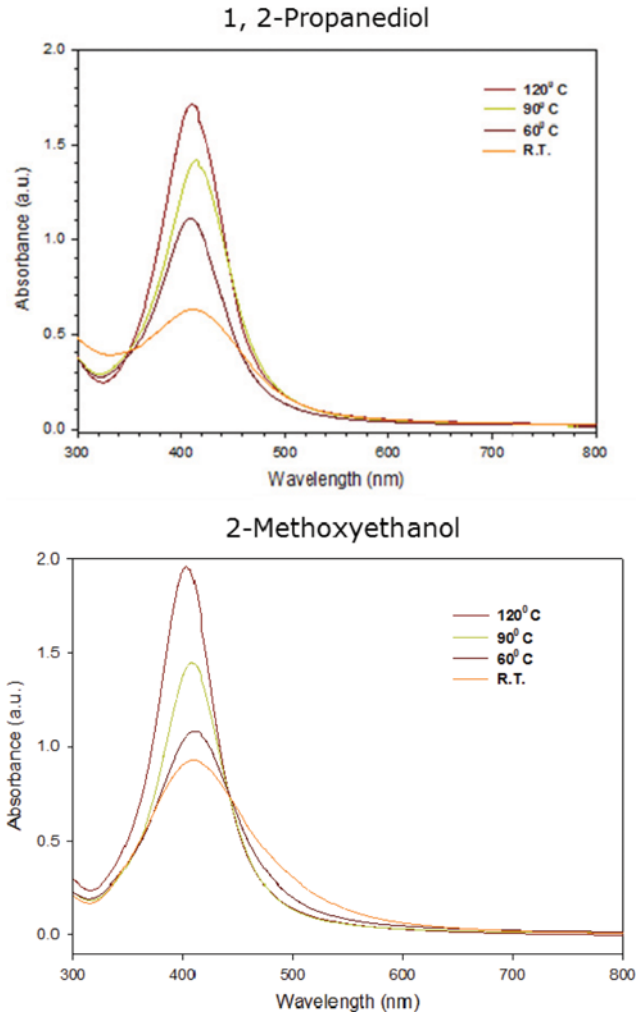

Fig. 7. Evolution of UV-vis absorption spectra after addition of ration PVP/$AgNO_3$ (24 : 1) in 1, 2-propanediol, 2-Methoxyethanol and heating at different temperature.

4. Effect of Temperature on Silver Nanoparticle Growth in 1, 2-Propanediol and 2-Methoxy Ethanol

The prepared samples were kept at the desired temperature for 30 min and were observed. The samples' coloration fast increased with temperature increment until a dark yellow. They presented the appearance of single surface plasmon resonance peak observed by UV-visible absorption spectroscopy with variation of intensity (Fig. 7). The variations of resonance peak intensity were found as similar as rising of temperature. The variation of intensity indicates the degree of advance of the reaction (reduction of Ag^+ at Ag^o) with the increase of the number of nanoparticles. In both solutions (1, 2-propanediol and 2-Methoxyethanol), the reduction rate to Ag^+ was found temperature dependent. The rate of reduction was much higher when the temperature was increased. The UV-visible spectrum of the yellow solution showed a well-defined surface plasmon resonance around 400 nm (Fig. 7). In fact, the energy of absorption would depend on the degree of plasmon resonance, i.e., it may shift to either side of this value depending on the ratio of silver ions and zero valent silver. The wavelength shift of the plasmon band position can be understood from simple Drude theory as a change in the free electron density of the particles which has relation with di-electric environment, particle size etc. [40]. Fig. 8 also shows the maximum peaks presented by silver nanoparticles, which are shifted by about 8 nm (blue shift) in comparison to the values between room temperature and 120 °C for 2-methoxyethanol. On the other hand, 1, 2-propanediol liquid showed a mixed phenomenon of blue and red shift. The red shift of the maximum absorption value is normally considered due to particle aggrega-

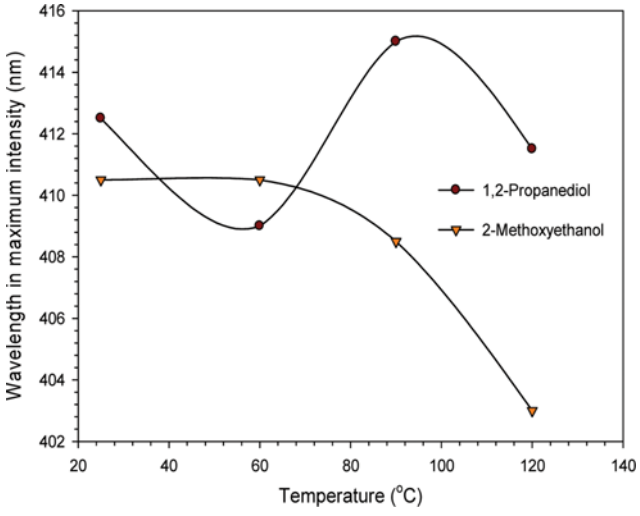

Fig. 8. Wavelength at maximum intensity with respect to different studied temperature of silver colloid in 1, 2-propanediol and 2-methoxyethanol.

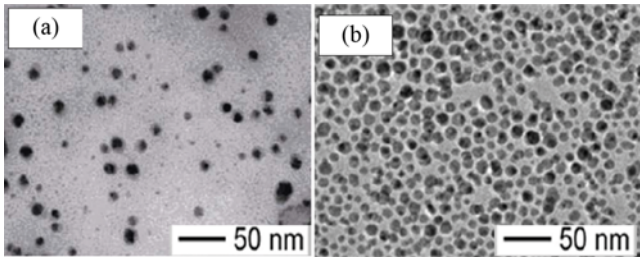

Fig. 9. TEM photographs of silver nanoparticles prepared in 1,2-propanediol (a), and 2-Methoxy ethanol (b) at 90 °C, respectively.

tion during the formation. The morphology of the solutions was studied by transmission electron microscopy (TEM) to determine shape and size of the nanoparticles. The outcomes clearly revealed that the resulting nanoparticles were isolated and not agglomerated (Fig. 9). The average sizes of nanoparticles were 11±3 nm (means± S.D.) and 20±5 nm (means±S.D.) for the respective liquids of 2-Methoxyethanol and 1, 2-propanediol. TEM results also supported this phenomenon where the particle size distribution becomes narrower in 2-methoxyethanol than 1, 2-propanediol. It seems that the sizes of the particle were potentially influenced by the polymer in the solution. It could be PVP/2-methoxyethanol colloid, which provides better film layer protection against aggregation than PVP/1, 2-propanediol colloid. The actual cause required further research on colloidal properties of the polymer and medium liquid. In this work, we confirmed that it is possible to obtain stable Ag nanoparticles in colloids using quite low concentration of PVP [39], much lower than the usual concentrations previously reported in the literature.

5. Zeta Potential and Stability of Silver Nanoparticle Colloid at Different Time Intervals

The ζ-potential value of the nanoparticles at the end of the reaction was determined to be −39.31 mV and −44.82 mV in 1, 2-propanediol and 2-methoxy ethanol, respectively. These values changed with time in a positive way. 2-methoxyethanol provides the higher negative potential than 1, 2-propandilo solvent. Large negative or positive values of the ζ-potential suggest a greater electrostatic repulsion between the nanoparticles, and there is no tendency of flocculation. Fig. 10 represents the ζ-potential change with time for two stable colloids prepared in 1, 2-propanedol and 2-methoxyethanol at 90 °C for four month. The particles in suspension with ζ-potential more positive than +30 mV or more negative than −30 mV are considered to be stable [41]. The particles charged similarly on the surface repelled each other due to electrostatic force of repulsion.

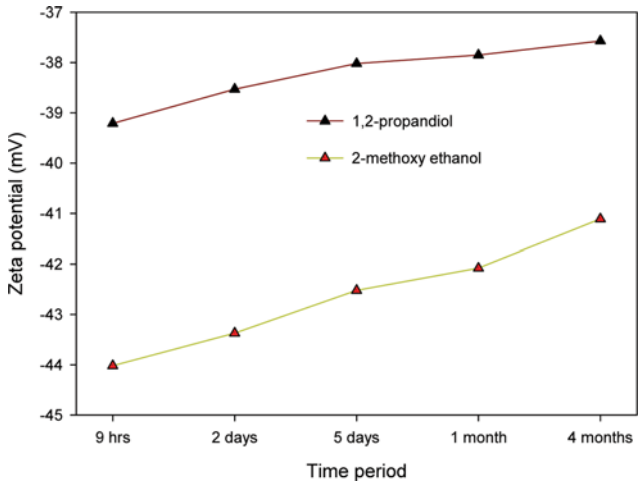

Fig. 10. Zeta potential of silver nanoparticle colloid in different time interval until four month prepared in 1, 2-propanediol and 2-methoxyethanol.

6. Effect on the Stability of Ag Nanoparticles with Varying Temperatures

Fig. 11(a) shows the absorbance spectra of solution reaction at room temperature (RT), 40, 60 and 90 °C, just prior to the final dark color transition. Before starting the agglomeration of silver nanoparticles it's called intermediate stage of the reaction as well as growth stage. Surface plasmon peak position is of 411 nm at RT and 40 °C, and 406 nm at 60 °C, 407 nm at 90 °C (Table 1). Fig. 11 indicates that the surface plasmon peak position does not change at RT and 40 °C, when a changes a little for 60 °C and 90 °C, but increases the height and shows that particles grow over time. According to the Drude model for dielectric properties, the Mei theory predicts that in the 6-10 nm particle size range the location of the surface plasmon peak does not change significantly, but the adsorption maximum grows [28]. However, the average particle size never exceeds a size required to shift the location of the surface plasmon peak. At the same time, another cause of these phenomena could be an increase in the number density of particles in the size range that exhibits a surface plasmon peak and change in the surface properties of the particle.

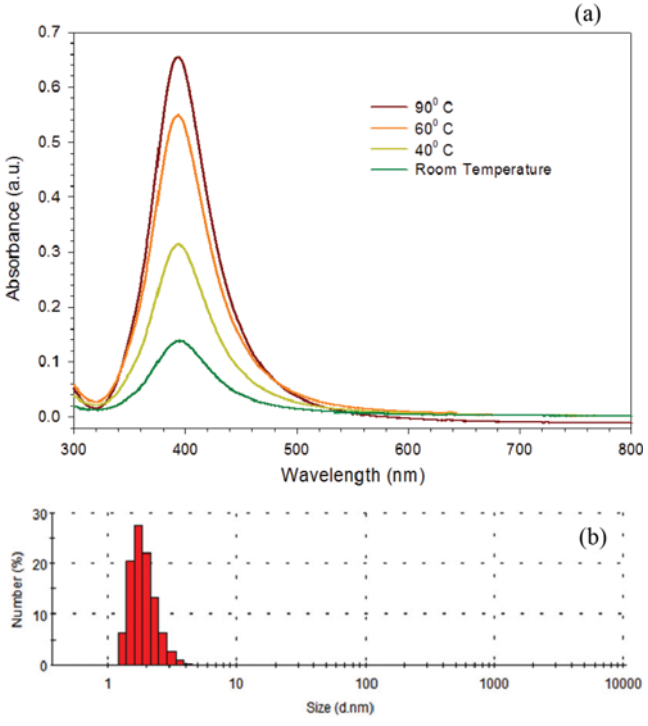

Fig. 11. The UV-vis spectra taken for the freshly prepared colloidal solutions at mentioned temperature. (a), size distribution of silver nanoparticles for 90 °C silver colloid (b).

At the end of the intermediate stage, particle size increases systematically from 6.0 nm to 18.0 nm as temperature increases from RT to 90 °C (Fig. 11(b)) with mean value of 9±3 nm. With the increase of temperature, the kinetic energy of silver nanoparticles in the solution increases; as a result, the collision frequency between the particles also rises and this leads to a higher rate agglomeration. As reported by Hyning and Zukoski [31], the surface potential of silver particles is inversely related to temperature. With increasing temperature, the gradual decrease in that potential of the particles accelerates the aggregation and thus the cluster formation, and as a result, increase of particle size, as observed in our case.

CONCLUSION

This research presented synthesis of silver nanoparticle in aqueous and organic medium with silver nitrate by sodium borohydride through a variety of embedded environment. The optical properties of silver nanoparticles were changed for the following components such as $AgNO_3$, $NaBH_4$, PVP and temperature in aqueous medium. The higher the applied parameter values, the more dispersed silver nano colloid with different movement of surface plasmon peak. Higher amount of PVP showed maximum blue shift movement by 13 nm of surface plasmon peak. Therefore, PVP application could be a more suitable choice to prepare more stable and non-aggregate silver colloids. 2-Methoxyethanol, an organic solvent showed a more blue shift on surface plasmon peak, more dispersed silver nanoparticles in TEM, and more negative zeta potential than 1, 2-propane diol. A comprehensive work on this solvent-particle interaction is needed in the future. Our study provides a context for understanding the stability of silver nanoparticles in aqueous and organic medium overall.

ACKNOWLEDGEMENT

This researh was supported by Basic Science Research Program through the National Research Foundation of Korea (NRF) funded by the Ministry of Science ICT & Future Planning (2017R1A2B4008720), and BK21 plus program in Republic of Korea.

REFERENCES

1. C. Shing, V. Sharma, P. Naik, V. Khandelwal and H. Singh, *Digest J. Nanomat Biostruct*, **6**(2), 535 (2011).
2. Y. Sun and Y. Xia, *Science*, **298**, 2176 (2002).
3. X. Wu, H. Liu, J. Liu, K. N. Haley, J. A. Treadway, J. P. Larson, E. Ge, F. Peale and M. P. Bruchez, *National Biotechnol.*, **21**, 41 (2003).
4. A. Ruivo, C. Gomes, A. Lima, M. L. Botelho, R. Melo, A. Belchior and A. P. Matos, *J. Cult. Herit*, **9**(Suppl.), e134 (2008).
5. O. Bobin, M. Schvoerer, C. Ney, M. Rammah, B. Pannequin, E. C. Platamone, A. Daoulatli and R. P. Gayraud, *Color Res. Appl.*, **28**, 352 (2003).
6. N. Asare, C. Instanes, W. J. Sandberg, M. Refsnes, P. Schwarze, M. Kruszewski and G. Brunborg, *Toxicology*, **291**(1-3), 65 (2011).
7. M. Ramos, D. A. Ferrer, R. R. Chianelli, V. Correa, J. M. Serrano and S. Flores, *J. Nanomaterials*, 1 (2011).
8. Y. Zheng, M. Xiao, S. Jiang, F. Ding and J. Wang, *Nanoscale*, **5**, 788 (2013).
9. B. Tang, J. F. Wang, S. P. Xu, T. Afrin, J. L. Tao, W. Q. Xu, L. Sun and X. Wang, *Chem. Eng. J.*, **185**, 366 (2012).
10. B. Tang, J. Li, X. Hou, T. Afrin, L. Sun and X. Wang, *Ind. Eng. Chem. Res.*, **52**, 4556 (2013).
11. P. Li, J. Li, C. Wu, Q. Wu and J. Li, *Nanotechnology*, **16**, 1912 (2005).
12. J. L. Elechiguerra, J. L. Burt, J. R. Morones, A. Camacho-Bragado, X. Gao, H. H. Lara and M. J. Yacaman, *J. Nanobiotechnol.*, **3**, 6 (2005), http://www.jnanobiotechnology.com/content/3/1/6.
13. R. Jin, Y. Cao, A. Mirkin, K. L. Kelly, G. C. Schatz and J. G. Zhang, *Science*, **294**, 1901 (2001).
14. R. A. de Barros, C. R. Martins and W. M. de Azevedo, *Synth. Met.*, **155**, 35 (2005), DOI:10.1016/j.synthmet.2005.05.014.
15. K. L. Kelly, E. Coronado, L. L. Zhao and G. C. Schatz, *J. Phys. Chem. B*, **107**, 668 (2002).
16. S. L. Kleinman, B. Sharma, M. G. Blaber, A.-I. Henry, N. Valley, R. G. Freeman, M. J. Natan, G. C. Schatz and R. P. V. Duyne, *J. Am. Chem. Soc.*, **135**, 301 (2013).
17. S. Szunerits and R. Boukherroub, *Chem. Commun.*, **48**, 8999 (2012).
18. A. I. Henry, J. M. Bingham, E. Ringe, L. D. Marks, G. C. Schatz and R. P. van Duyne, *J. Phys. Chem. C*, **115**, 9291 (2011).
19. L. M. L. Marzan and I. Lado-Tourino, *Langmuir*, **12**(15), 3585 (1996).
20. A. K. Rashid, R. K. Renat, G. Olga, E. Yuri and S. Thomas, *Nanopart. Res.*, **11**, 1193 (2009).
21. A. B. Smetana, K. J. Klabunde and C. M. Sorensen, *J. Colloid Interface Sci.*, **284**(2), 521 (2005).
22. K. J. Lee, B. H. Jun, J. Choi, Y. I. Lee, J. Joung and Y. S. Oh, *Nanotechnology*, **18**, 335601 (5pp) (2007).
23. P. Y. Silvert, R. Herrera-Urbina, N. Duvauchelle and V. Vijayakrishnan, *J. Mater. Chem.*, **6**(4), 573 (1996).
24. Y. P. Sun, P. Atorngitjawat and M. J. Meziani, *Langmuir*, **17**(19), 5707 (2001).
25. A. Henglein, *Chem. Mater.*, **10**(1), 444 (1998).
26. T. Kaushik, S. Mhatre and R. Parikh, *Nanomed Nanotechnol. Bio. Med.*, **6**(2), 257 (2010).
27. K. D. Kim, D. N. Han and H. T. Kim, *Chem. Eng. J.*, **104**, 55 (2004).
28. H. D. L. Van and C. F. Zukoski, *Langmuir*, **14**, 7034 (1998).
29. J. P. Chen and L. L. Lim, *Chemosphere*, **49**(4), 363 (2002).
30. A. Tao, P. Sinsermsuksaku and P. Yang, *Angew. Chem. Int.*, **45**, 4597 (2006).
31. H. D. L. Van and C. F. Zukoski, *Langmuir*, **17**, 3128 (2001).
32. G. Wang, C. Shi, N. Zhao and X. Du, *Mater. Lett.*, **61**, 3795 (2007).
33. K. C. Song, S. M. Lee, T. S. Park and B. S. Lee, *Korean J. Chem. Eng.*, **26**(1), 153 (2009).
34. J. Liu, J. B. Lee, D. H. Kim and Y. Kim, *Colloids Surf., A*, **302**, 276 (2007).
35. S. D. Solomon, M. Bahadory, A. V. Jeyarajasingam, S. A. Rutkowsky and C. Boritz, *J. Chem. Ed.*, **84**, 322 (2007).
36. J. Eastman and T. Cosgrove, Ed., p. 54, Blackwell UK (2005).
37. T. L. Farias., U. O. Koylu and M. G. *J. Quant. Spectrosc. Radiar. Transfer.*, **55**(3), 357 (1996).
38. W. R. Glomm, *J. Dispersion Sci. Technol.*, **26**, 389 (2005).
39. Victor Elias Torres Heredia, doctoral thesis (2011).
40. K. B. Mogensen and K. Kneipp, *J. Phys. Chem. C*, **118**, 28075 (2014).
41. S. S. Khan, A. Mukherjee and N. Chandrasekaran, *Water Res.*, **45**, 5184 (2011).